Title	Near-infrared electroluminescent devices based on colloidal HgTe quantum dot arrays
Authors	O'Connor, Éamon;O'Riordan, Alan;Doyle, Hugh;Moynihan, Shane;Cuddihy, Aoife;Redmond, Gareth
Publication date	2005-05
Original Citation	O'CONNOR, É., O'RIORDAN, A., DOYLE, H., MOYNIHAN, S., CUDDIHY, A. & REDMOND, G. 2005. Near-infrared electroluminescent devices based on colloidal HgTe quantum dot arrays. Applied Physics Letters, 86, 201114. DOI: 10.1063/1.1928321
Type of publication	Article (peer-reviewed)
Link to publisher's version	http://scitation.aip.org/content/aip/journal/apl/86/20/10.1063/1.1928321 - 10.1063/1.1928321
Rights	Copyright 2005 American Institute of Physics. This article may be downloaded for personal use only. Any other use requires prior permission of the author and the American Institute of Physics. The following article appeared in Applied Physics Letters, 86, 201114 (2005) and may be found at http://scitation.aip.org/content/aip/journal/apl/86/20/10.1063/1.1928321
Download date	2024-12-29 07:34:55
Item downloaded from	https://hdl.handle.net/10468/1644

Near-infrared electroluminescent devices based on colloidal HgTe quantum dot arrays

É. O'Connor, A. O'Riordan, H. Doyle, S. Moynihan, A. Cuddihy, and G. Redmond[a]
Nanotechnology Group, Tyndall National Institute, Lee Maltings, Prospect Row, Cork, Ireland

Crystalline 4.6 nm HgTe quantum dots, stabilized by 1-thioglycerol ligands, were synthesized by wet chemical methods. Room-temperature photoluminescence spectra of the dots, both in solution and as solid arrays, exhibited near-infrared emission. Light-emitting devices were fabricated by deposition of quantum dot layers onto glass/indium tin oxide (ITO)/ 3,4-polyethylene-dioxythiophene-polystyrene sulfonate (PEDOT) substrates followed by top contacting with evaporated aluminum. Room-temperature near-infrared electroluminescence from 1 mm^2 ITO/PEDOT/HgTe/Al devices, centered at ∼1600 nm, with an external quantum efficiency of 0.02% and brightness of 150 nW/mm^2 at 50 mA and 2.5 V was achieved. © *2005 American Institute of Physics.* [DOI: 10.1063/1.1928321]

Chemically synthesized colloidal nanocrystals (quantum dots) exhibit many attractive physical properties, from size-tunable optical and electronic properties to versatile solution processability.[1] In the field of photonics, these characteristics have provided opportunities for the exploitation of colloidal quantum dots based on materials, such as CdS, ZnS, CdSe, and CdTe, in applications as diverse as biolabeling, photovoltaics, electroluminescence, optical amplification, and stimulated emission.[2–7] In recent years, in order to explore their potential for use at telecommunications wavelengths, efforts have been made to extend the optical response of colloidal quantum dots from the visible to the near-infrared (NIR) by the synthesis of nanocrystals based on, e.g., InAs, PbS, PbSe, and HgTe.[8–12] As a result, an initial demonstration of phenomena, such as size-tunable NIR luminescence, electroluminescence (EL) and optical gain, has been possible.[13–17]

Concerning HgTe, in particular, this material has an inverted band structure and an essentially negative band gap of around −0.15 eV at 295 K.[18] It is expected that the effect of quantum confinement in HgTe quantum dots should increase the effective band gap of the material and give rise to NIR luminescence. To address this issue, colloidal HgTe quantum dots were recently synthesized in an aqueous solution at room temperature by wet chemical means, and were shown to be very stable toward oxidation due to effective surface passivation.[11,12,19] The dots exhibited room-temperature photoluminescence (PL) covering the 1.3 μm and 1.55 μm telecommunications windows with emission wavelength dependence upon synthetic conditions and with extremely high quantum efficiencies of up to 50%. Given the potential for the future realization of low cost solution processable electrically pumped NIR optical emitters and amplifiers presented by such materials, in this letter we report on the fabrication of devices based on arrays of colloidal HgTe nanocrystals where EL in the 1.3 to 1.7 μm region is achieved by the injection of charge carriers directly into the quantum dot solid.

1-thioglycerol-stabilized colloidal HgTe quantum dots were prepared in an aqueous solution at room temperature using the method described previously.[11] 1-thioglycerol is an effective size-regulating and stabilizing agent for II-VI semiconductor nanocrystals allowing the efficient recovery of crystallites in powder form following synthesis (by precipitation with propan-2-ol) and also redispersion of the nanocrystals in solvents of choice. Mercury (II) perchlorate, dimethylformamide (DMF), and 1-thiogycerol were purchased from Aldrich Ltd. Aluminum telluride and propan-2-ol were purchased from Cerac Inc. and Rockwood Electronic Materials, respectively. All reagents were used as received. Aqueous colloidal HgTe quantum dot dispersions were prepared by passing hydrogen telluride gas through a N$_2$-saturated aqueous mercury (II) perchlorate solution at pH 10.0 in the presence of 1-thioglycerol as a stabilizing agent. Propan-2-ol was then added, drop wise, to induce turbidity and the solution was stirred for 2–3 h. The 1-thioglycerol-capped HgTe dots were separated by centrifugation (6000 rpm; 10 min) and redispersed in 500 μl of deionized water or DMF, with 2.5 μl of 1-thioglycerol added to ensure complete dispersion. In a typical synthesis, a 12 mg/ml dispersion of 1-thioglycerol-capped quantum dots was obtained.

Solution-phase ultraviolet-visible (UV-VIS) and PL spectra were recorded using a 1:50 dilution of the stock aqueous colloidal quantum dot dispersion. Arrays of HgTe quantum dots were prepared for PL characterization by drop depositing a 5 μl aliquot of nanocrystals in DMF onto clean glass cover slips and drying under ambient conditions (30 min). Absorbance spectra were measured using an UV-VIS diode array spectrometer (Agilent 8453). PL spectra were measured using a custom-built measurement system, incorporating an argon-ion laser (488 nm excitation wavelength) and monochromator with a resolution of 0.1 nm. NIR light was detected with a liquid-nitrogen-cooled Ge detector. Samples for electron microscopy and powder x-ray diffraction (XRD) analysis were prepared by dropcasting 1 mg/ml of aqueous dispersions of the dots onto 400-mesh carbon-coated Formvar®/copper grids and cleaned microscope slides, respectively, with the excess solvent removed immediately. High-resolution transmission electron microscopy (HRTEM) images were recorded using a Jeol JEM-2011

[a]Author to whom correspondence should be addressed; electronic mail: gareth.redmond@tyndall.ie
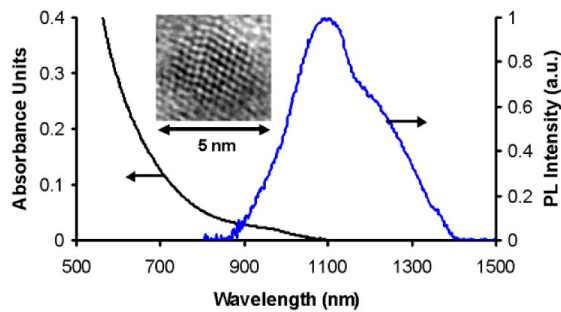
FIG. 1. (Color online) UV-VIS absorption and PL spectra of freshly prepared HgTe quantum dots dispersed in water. Inset: HRTEM image of a single dot showing well-resolved lattice planes.
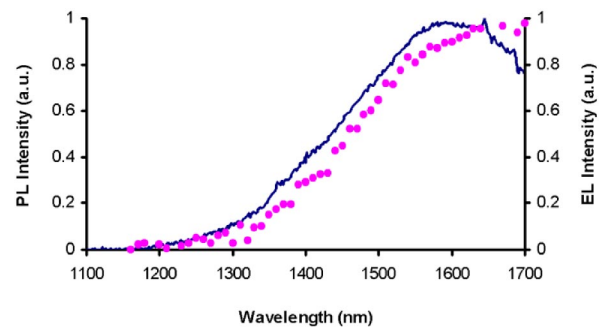

FIG. 2. (Color online) PL spectrum (solid line) of a HgTe quantum dot array deposited on a glass substrate and the EL spectrum (solid circles) acquired from a HgTe quantum dot device. Inset: Schematic of the ITO/PEDOT/HgTe/Al device structure employed (not to scale).

transmission electron microscope. Powder XRD patterns were measured on a Philips PW3710 diffractometer using Cu Kα radiation.

EL device substrates comprised of indium tin oxide (ITO) electrodes (sheet resistance of 10 Ω) lithographically patterned to define a 1 mm^2 device area on glass. Substrates were prepared by cleaning with a solvent wash and oxygen plasma (50 W, 1 bar, 5 min), followed by deposition of a typically 70 nm thick layer of 3,4-polyethylene-dioxythiophene-polystyrene sulfonate (PEDOT:PPS) (Baytron P, VP AI 4083) by spincasting. HgTe quantum dot layers were drop deposited from DMF solution onto each device anode in a controlled atmosphere glovebox, allowed to dry (30 min; 25 °C), and then annealed under a vacuum (45 min; 90 °C). Batch-to-batch film thickness was measured at ~100 nm. To complete device fabrication, a low work function cathode, aluminum (300 nm), was thermally evaporated at a rate of 2 Å/s, under a vacuum of 3×10^{-7} mbar. Current-voltage-luminance ($I/V/L$) characteristics of fabricated devices were measured under inert atmosphere conditions using a dc power supply with a calibrated germanium photodiode connected to an optical power meter. Emitted light was collected with the detector placed directly in contact with the back side of the device. Optical corrections for absorption, wave guiding, or other effects that reduced the light emitted from a device were not considered in the measurements. EL spectra were measured under ambient conditions using a calibrated integrating sphere. To prevent device degradation, devices were encapsulated in a protective epoxy.

HRTEM analysis of 1-thioglycerol-capped HgTe nanocrystals yielded an average nanocrystal size of 4.6 nm, with a polydispersity, $\sigma \sim 16\%$. The well-resolved lattice planes discernible in images of single nanocrystals indicated a high degree of crystallinity; see Fig. 1 (inset). Analysis of XRD data acquired from HgTe nanocrystal powder samples indicated that the crystal structure derived from the positions of the wide-angle diffraction peaks was the cubic (F$\bar{4}$3m) phase of bulk HgTe (coloradoite).[20] Also, Scherrer analysis of the full widths at half maximum (FWHM) of the (111), (220), and (311) reflections yielded a mean crystallite diameter of ~4.6 nm. Together, the HRTEM and XRD data confirmed the formation of highly crystalline, single-domain 4.6 nm HgTe quantum dots.

Figure 1 shows UV-VIS absorption and PL spectra of freshly synthesized nanocrystals acquired immediately following redispersion in deionized water. The absorption spectrum exhibited a weak maximum at 960 nm attributed to the

lowest level excitonic absorption, with increasing absorbance at shorter wavelengths.[11,12] The PL spectrum, assigned to recombination of photogenerated charge carriers on the dots, exhibited a broad emission band from 900 to 1400 nm with an intensity maximum at 1090 nm.[19] The broad PL spectral width (FWHM ~260 nm) was a result of inhomogeneous broadening due to the HgTe nanocrystal size distribution. Water reabsorption was responsible for the small dip or shoulder observed in the PL spectrum at 1150 nm and also for the cutoff of the spectrum at 1450 nm. The PL spectrum measured from a HgTe quantum dot array drop deposited onto a glass cover slip from DMF also displayed strong NIR emission with an emission maximum of 1590 nm, i.e., covering almost the entire 1.55 μm telecommunications window; see Fig. 2. Acquisition of PL spectra in this manner eliminated complications due to water reabsorption thereby simplifying the measurement of quantum dot emission. While redshifted emission from HgTe nanocrystals in a solution is attributed to nanocrystal ripening or particle ageing, the PL redshift that occurred on going from a colloidal dispersion to a closely packed quantum dot array, as shown in Fig. 2, suggests the further involvement of proximity-enhanced interdot coupling effects that facilitate energy transfer from smaller to larger nanocrystals.[19,21,22]

Concerning the possibility of observing EL from such HgTe quantum dot arrays, infrared emission was detected from ITO/PEDOT/HgTe/Al devices fabricated as described above; see Fig. 2. EL spectra of the devices exhibited a similar profile to the PL spectra of drop deposited arrays. The near coincidence of the electrically and optically generated spectra demonstrates that, in both cases, the same emissive species were responsible for the luminescence. However, the EL spectrum was redshifted by approximately 70 nm compared to the PL spectrum with an intensity maximum at ~1660 nm. Redshifts in EL emission spectra compared to PL spectra have been observed in visible-emitting devices based on CdSe/CdS core/shell nanocrystals doped into poly(paraphenylene vinylene) hosts, and attributed mainly to the reabsorption of a portion of the EL within the nanocrystal layer.[23] A redshift could also result from nanocrystal charging, the presence of strong electric fields within the device during operation, or from size selection in the EL due to either Förster energy transfer from smaller to larger nanocrystals or the existence of a smaller barrier to charge injection into larger nanocrystals. Notably, similar spectral shifts between PL and EL were recently reported for NIR-emitting devices based on InAs/ZnSe core/shell nanocrystals embed-
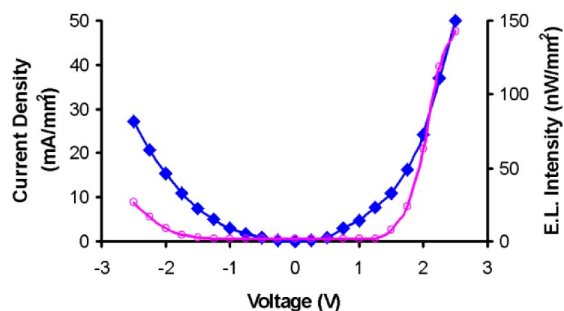
FIG. 3. (Color online) Typical $I/V/L$ characteristics of a NIR-emissive HgTe quantum dot device (ITO/PEDOT/HgTe/Al). Solid diamonds: Current; open circles: NIR luminance.

ded in poly(2-methoxy-5-(2′-ethyl-hexyloxy)-1,4 phenylene vinylene matrices and attributed to energy transfer from smaller to larger nanocrystals.[13]

Current-voltage curves of ITO/PEDOT/HgTe/Al devices indicated non-Ohmic and slightly rectifying behavior; see Fig. 3. EL was observed in both forward and reverse bias. The mechanism for light emission is likely based on the direct injection of charge carriers into the nanocrystals followed by recombination, consistent with the short length of the 1-thioglycerol-stabilizing ligands.[14,15] It was observed that the threshold voltage for light emission for devices at forward bias ($\sim$1 V) was lower than that measured for devices at reverse bias ($\sim$1.4 V). Also, the EL intensity measured from devices at forward bias was almost five times higher than that measured for devices at reverse bias; see Fig. 3. The reduced luminescence intensity observed for devices at reverse bias suggests that the energy barrier for electron injection at the PEDOT/nanocrystal interface, under this bias condition, is higher than that for electron injection at the Al/nanocrystal interface at forward bias. Similar behavior has been previously observed in visible-emitting devices incorporating CdSe/ZnS core/shell nanocrystal layers deposited on PEDOT and accounted for in this manner.[24] A maximum external quantum efficiency of 0.02% and a maximum light output of 150 nW/mm^2 at 50 mA and 2.5 V were measured for the 1 mm^2 ITO/PEDOT/HgTe/Al devices. This measured external quantum efficiency is an order of magnitude higher than that reported for NIR-emitting organic light-emitting diode devices fabricated using HgTe dots blended into a conjugated polymer matrix.[16] This efficiency also represents a minimum value as no optical corrections were made for absorption, wave guiding, or other effects that might reduce light output, e.g., ITO reabsorption ($a \sim 100$ nm thick ITO film has only 70% transparency at 1500 nm).[15]

In summary, EL devices based on colloidal HgTe quantum dot arrays have been fabricated. Room-temperature NIR emission in the 1.3 to 1.7 μm region, due to the direct injection of charge carriers into the quantum dots, has been ob-

served. It is expected that future improvements in materials processing, device design, and device fabrication will permit the optimization of the performance of these NIR-emissive devices, and will also provide opportunities to explore their applicability in telecommunications and other key photonics applications.

[1] M. Nirmal and L. E. Brus, Acc. Chem. Res. **30**, 475 (1999).
[2] W. C. W. Chan and S. Nie, Science **281**, 2016 (1998).
[3] N. C. Greenham, X. G. Peng, and A. P. Alivisatos, Phys. Rev. B **54**, 17628 (1996).
[4] V. C. Colvin, M. C. Schlamp, and A. P. Alivisatos, Nature (London) **370**, 354 (1994).
[5] S. Coe, W.-W. Woo, M. Bawendi, and V. Bulović, Nature (London) **420**, 800 (2002).
[6] V. I. Klimov, A. A. Mikhailovsky, S. Xu, A. Malko, J. A. Hollingsworth, C. A. Leatherdale, H.-J. Eisler, and M. G. Bawendi, Science **290**, 314 (2000).
[7] S. A. Ivanov, J. Nanda, A. Piryatinski, M. Achermann, L. P. Balet, I. V. Bezel, P. O. Anikeeva, S. Tretiak, and V. J. Klimov, J. Phys. Chem. B **108**, 10625 (2004).
[8] Y. W. Cao and U. Banin, J. Am. Chem. Soc. **122**, 9692 (2000).
[9] L. Bakueva, I. Gorelikov, S. Musikhin, X. S. Zhao, and E. H. Sargent, Adv. Mater. (Weinheim, Ger.) **16**, 926 (2004).
[10] J. M. Pietryga, R. D. Schaller, D. Werder, M. H. Stewart, V. I. Kilmov, and J. A. Hollingsworth, J. Am. Chem. Soc. **126**, 11752 (2004).
[11] A. Rogach, S. Kershaw, M. Burt, M. Harrison, A. Kornowski, A. Eychmüller, and H. Weller, Adv. Mater. (Weinheim, Ger.) **11**, 552 (1999).
[12] M. T. Harrison, S. V. Kershaw, A. L. Rogach, A. Kronowski, A. Eychmüller, and H. Weller, Adv. Mater. (Weinheim, Ger.) **12**, 123 (2000).
[13] N. Tessler, V. Medvedev, M. Kazes, S. Kan, and U. Banin, Science **295**, 1506 (2002).
[14] L. Bakueva, S. Musikhin, M. A. Hines, T-W. F. Chang, M. Tzolov, G. D. Scholes, and E. H. Sargent, Appl. Phys. Lett. **82**, 2895 (2003).
[15] J. S. Steckel, S. Coe-Sullivan, V. Bulović, and M. G. Bawendi, Adv. Mater. (Weinheim, Ger.) **15**, 1862 (2003).
[16] D. S. Koktysh, N. Gaponik, M. Reufer, J. Crewet, U. Scherf, A. Eychmüller, J. M. Lupton, A. L. Rogach, and J. Feldmann, ChemPhysChem **5**, 1435 (2004).
[17] R. D. Schaller, M. A. Petruska, and V. I. Klimov, J. Phys. Chem. B **107**, 13765 (2003).
[18] Landolt–Börnstein, *Numerical Data and Functional Relationships in Science and Technology*, New Series Vol. 17b: Semiconductors (Springer, Berlin 1982).
[19] M. T. Harrison, S. V. Kershaw, M. G. Burt, A. Rogach, A. Eychmuller, and H. Weller, J. Mater. Chem. **9**, 2721 (1999).
[20] Card No. 981, Mineral Crystal Structure Database, Institute of Experimental Mineralogy, Chernogolovka, Russia.
[21] C. B. Murray, C. R. Kagan, and M. G. Bawendi, Science **270**, 1335 (1995).
[22] C. R. Kagan, C. B. Murray, and M. G. Bawendi, Phys. Rev. B **54**, 8633 (1996).
[23] M. C. Schlamp, X. Peng, and A. P. Alivisatos, J. Appl. Phys. **82**, 5837 (1997).
[24] R. A. M. Hikmet, D. V. Talapin, and H. Weller, J. Appl. Phys. **93**, 3509 (1998).